

# Out-of-equilibrium open quantum systems: A comparison of approximate quantum master equation approaches with exact results

Archak Purkayastha and Abhishek Dhar

*International Center for Theoretical Sciences, Tata Institute of Fundamental Research, Bangalore 560012, India*

Manas Kulkarni

*Department of Physics, New York City College of Technology, The City University of New York, Brooklyn, New York 11201, USA*

(Received 17 December 2015; published 13 June 2016)

We present the Born-Markov approximated Redfield quantum master equation (RQME) description for an open system of noninteracting particles (bosons or fermions) on an arbitrary lattice of  $N$  sites in any dimension and weakly connected to multiple reservoirs at different temperatures and chemical potentials. The RQME can be reduced to the Lindblad equation, of various forms, by making further approximations. By studying the  $N = 2$  case, we show that RQME gives results which agree with exact analytical results for steady-state properties and with exact numerics for time-dependent properties over a wide range of parameters. In comparison, the Lindblad equations have a limited domain of validity in nonequilibrium. We conclude that it is indeed justified to use microscopically derived full RQME to go beyond the limitations of Lindblad equations in out-of-equilibrium systems. We also derive closed-form analytical results for out-of-equilibrium time dynamics of two-point correlation functions. These results explicitly show the approach to steady state and thermalization. These results are experimentally relevant for cold atoms, cavity QED, and far-from-equilibrium quantum dot experiments.

DOI: [10.1103/PhysRevA.93.062114](https://doi.org/10.1103/PhysRevA.93.062114)

## I. INTRODUCTION

Understanding out-of-equilibrium quantum systems, both bosonic and fermionic, has been of great experimental and theoretical interest recently. Such open quantum systems have been realized both in the bosonic case (experiments on cavity-QED arrays [1–4], cold atoms [5,6], cavity optomechanics [7,8]) and in the fermionic case (nonequilibrium transport in coupled quantum dots [1,9–12], cold atoms [13]). A typical setup of interest (see Fig. 1) is a system of a small number of bosonic (fermionic) degrees of freedom coupled to a bosonic (fermionic) bath or environment composed of a large number of degrees of freedom. The general case can be defined as a scenario in which each degree of freedom of the subsystem is coupled to a bath characterized by a temperature  $T = 1/\beta$  and a chemical potential  $\mu$ . New cutting-edge technologies available recently for measuring physical quantities such as occupation number, currents, and correlations in such systems make it of paramount importance to develop an approach that produces accurate results. Additionally, these open quantum systems are widely tunable, thereby providing a large window of parameters to test the validity of different approaches.

One of the most commonly used frameworks in the study of open quantum systems in the limit of weak system-bath coupling is the quantum master equation (QME) method, where one writes a time-evolution equation for the reduced density matrix  $\rho$  of the system. Two QMEs that are popular in the literature are the Redfield [14] and the Lindblad equations [15,16]. The Redfield equations (RQME) are obtained under the so-called Born-Markov approximation (see below). After further approximations and depending on the nature of these, we get either the local coordinate basis (site-basis) Lindblad QME (LLQME) or the eigenfunction basis Lindblad QME (ELQME). An advantage of the Lindblad equations is that they have been proven to preserve positivity of  $\rho$ . Hence,

they are widely used in the literature [17–29]. However, both Lindblad equations are known to have limitations. The local-basis Lindblad does not give the correct thermalization [27,28] for noninteracting bosons or fermions, while the eigenbasis Lindblad gives zero particle current inside the system even in the nonequilibrium steady state (NESS) [27,29].

The RQME provides an alternative. It has been previously used to find NESS properties in open quantum harmonic chains, spin chains, and fermionic lattices [30–38]. RQME is known to give thermalization but is more difficult to solve both numerically and analytically. Also, it does not guarantee the complete positivity of the system density matrix at all times. This may lead to various subtle pathologies depending on initial conditions, as shown in some recent works [39,40]. The Lindblad equations, on the other hand, are free from these pathologies.

Because of such inherent pathologies and limitations stemming from the approximations, it is important to check the performance of the approximate QMEs against exact results. Results from RQME, Lindblad QMEs, and exact calculations have recently been compared for a single oscillator in NESS [41] and for a two-site bosonic problem in equilibrium [42]. To our knowledge, rigorous checks have not been performed for multiple sites in nonequilibrium.

In this paper, we ask the question whether adopting RQME to go beyond the limitations of the Lindblad methods in nonequilibrium systems is justified. To this end, first, for an out-of-equilibrium system of noninteracting bosons or fermions in an arbitrary lattice of  $N$  sites in any dimension, we derive a closed set of linear differential equations for two-point correlation functions from RQME. Such a closed set of linear differential equations can be easily solved numerically. This therefore gives a numerical way to compute physical results for such out-of-equilibrium systems from RQME. Next, to

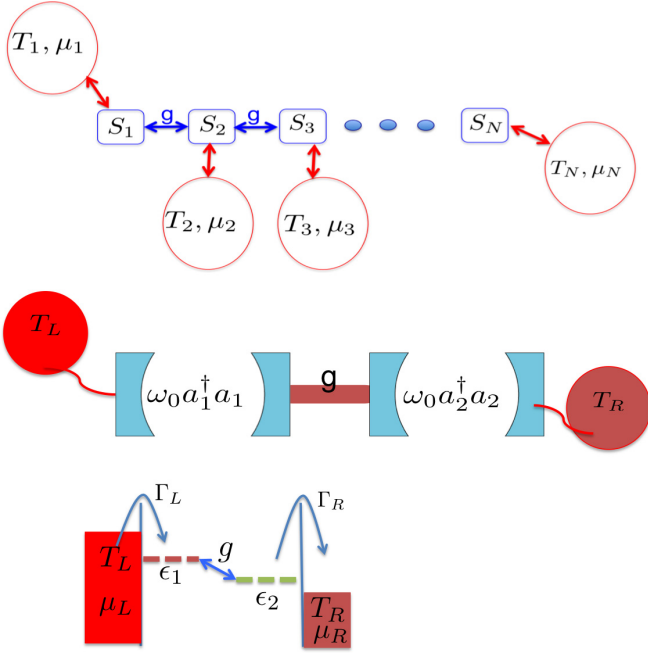


FIG. 1. A schematic of the setup we consider. We have a system of  $N$  lattice sites with noninteracting particles on them. Each site of the system is coupled to its respective bath of a chosen temperature and chemical potential. Baths out of equilibrium can facilitate transport. The top diagram is general for the bosonic or fermionic case, and such situations have been realized experimentally in setups such as those given in the middle and bottom diagrams.

check the validity of such solutions, we compute the physical quantities of interest from RQME for a system of two bosonic or fermionic modes connected to two baths at different temperatures and chemical potentials (i.e., out of equilibrium) and compare them against exact results obtained from other open-system approaches, such as the quantum Langevin method (QLE), where exact equations for system degrees of freedom admit the form of an effective generalized Langevin equation, and the equation-of-motion (EOM) method [43–46]. We find that RQME indeed reproduces the exact results quite accurately. We also provide closed-form analytical results for out-of-equilibrium time dynamics of two-point correlation functions for the two-site problem. Throughout the paper,  $\hbar$  is taken to be unity.

The plan of the paper is as follows. In Sec. II we define the general model and give a derivation of the Redfield QME. In Sec. III we consider a two-site example and compare results obtained from different QMEs with exact results. Finally, we summarize our results in Sec. IV.

## II. THE MODEL AND THE REDFIELD QME (RQME)

### A. Definition of the model

We consider noninteracting bosonic (fermionic) particles on a lattice of  $N$  sites in arbitrary dimension and of arbitrary geometry where each site is coupled to bosonic (fermionic) baths. The bath Hamiltonian  $\hat{\mathcal{H}}_B$  and the coupling between system and baths  $\hat{\mathcal{H}}_{SB}$  are taken to be bilinear. The full

Hamiltonian thus takes the form

$$\begin{aligned} \hat{\mathcal{H}} &= \hat{\mathcal{H}}_S + \hat{\mathcal{H}}_B + \hat{\mathcal{H}}_{SB}, \\ \hat{\mathcal{H}}_S &= \sum_{\ell=1}^N H_{\ell m}^{(S)} \hat{a}_\ell^\dagger \hat{a}_m, \quad \hat{\mathcal{H}}_B = \sum_{\ell=1}^N \sum_{r=1}^{\infty} \Omega_r^\ell \hat{B}_r^{\ell\dagger} \hat{B}_r^\ell, \\ \hat{\mathcal{H}}_{SB} &= \varepsilon \sum_{\ell=1}^N \sum_r (\kappa_{\ell r} \hat{B}_r^{\ell\dagger} \hat{a}_\ell + \kappa_{\ell r}^* \hat{a}_\ell^\dagger \hat{B}_r^\ell), \end{aligned} \quad (1)$$

where  $H^{(S)}$  is a Hermitian matrix and  $\hat{a}_\ell$  corresponds to bosonic (fermionic) annihilation operators defined on the  $\ell$ th lattice point of the system and  $\hat{B}_r^\ell$  corresponds to those of baths attached to the  $\ell$ th point. The baths have infinite degrees of freedom.  $\varepsilon$  is a parameter that controls system-bath coupling and has dimensions of energy, so that  $\{\kappa_{\ell r}\}$  are dimensionless and  $O(1)$ . We assume that, initially, each of the  $\ell$  baths is at thermal equilibrium at its own inverse temperature  $\beta_\ell$  and chemical potential  $\mu_\ell$ , and there is no coupling between system and baths. Thus, the initial bath correlation functions satisfy the thermal properties:

$$\langle \hat{B}_r^\ell \rangle = 0, \quad \langle \hat{B}_r^{\ell\dagger} \hat{B}_s^\ell \rangle_B = n_\ell(\Omega_r^\ell) \delta_{rs}, \quad (2)$$

where  $n_\ell(\omega) = [e^{\beta_\ell(\omega - \mu_\ell)} \pm 1]^{-1}$  is the fermionic or bosonic distribution function. We also introduce the bath spectral functions:

$$J_\ell(\omega) = 2\pi \sum_r |\kappa_{\ell r}|^2 \delta(\omega - \Omega_r^\ell). \quad (3)$$

### B. Redfield QME

In the Redfield approach, one assumes a weak-system-bath-coupling limit. Performing the Born-Markov approximation leads to the standard Redfield equation [47,48]. For bilinear system-bath coupling  $\hat{\mathcal{H}}_{SB} = \sum_\ell \hat{S}_\ell \hat{B}_\ell$ , where  $\hat{S}_\ell$  operates on the system and  $\hat{B}_\ell$  operates on the bath, with system-bath coupling being turned on at time  $t = 0$ , we have the master equation

$$\begin{aligned} \frac{\partial \rho^I}{\partial t} &= - \sum_{\ell, m} \int_0^t dt' \{ [\hat{S}_\ell^I(t), \hat{S}_m^I(t')] \rho^I(t) \} \langle \hat{B}_\ell^I(t) \hat{B}_m^I(t') \rangle_B \\ &+ [\rho^I(t) \hat{S}_m^I(t'), \hat{S}_\ell^I(t)] \langle \hat{B}_m^I(t') \hat{B}_\ell^I(t) \rangle_B, \end{aligned} \quad (4)$$

where we use the interaction representation  $\hat{O}^I(t) = e^{i(\hat{\mathcal{H}}_S + \hat{\mathcal{H}}_B)t} \hat{O} e^{-i(\hat{\mathcal{H}}_S + \hat{\mathcal{H}}_B)t}$  and  $\langle \dots \rangle_B$  refers to the average taken only with respect to the bath. In order to obtain the explicit QME for our model, it is convenient to go to the eigenbasis of the system Hamiltonian. Let  $c$  be the unitary matrix which diagonalizes  $H^{(S)}$ , i.e.,

$$c^\dagger H^{(S)} c = \omega^{(D)}, \quad (5)$$

where  $c^\dagger c = I$  and  $\omega^{(D)}$  is a diagonal matrix with elements  $\omega_\nu$ . Then we also define new operators  $\{A_\alpha\}$  through the transformation

$$\hat{a}_\ell = \sum_{\alpha=1}^N c_{\ell\alpha} \hat{A}_\alpha. \quad (6)$$

Thus,  $\hat{A}_\alpha$  is the annihilation operator for the  $\alpha$ th eigenmode with energy  $\omega_\alpha$ . For RQME to be valid, we choose  $\varepsilon \ll \{\omega_\alpha\}$ .

After some tedious algebra (see the Appendix), we obtain our QME for the reduced density matrix  $\rho$  of the system:

$$\begin{aligned} \frac{\partial \rho}{\partial t} &= i[\rho, H_S] - \varepsilon^2 \sum_{\alpha, \nu=1}^N \int \frac{d\omega}{\pi} \left[ \int_0^\infty d\tau e^{i(\omega - \omega_\nu)\tau} \mathcal{L}(\hat{A}_\alpha^\dagger, \hat{A}_\nu; \omega) \rho + \text{H.c.} \right], \\ \mathcal{L}(\hat{A}_\alpha^\dagger, \hat{A}_\nu; \omega) \rho &= [f_{\alpha\nu}(\omega) \mp F_{\alpha\nu}(\omega)] [\hat{A}_\alpha^\dagger, \hat{A}_\nu \rho] + F_{\alpha\nu}(\omega) [\rho \hat{A}_\nu, \hat{A}_\alpha^\dagger], \\ f_{\alpha\nu}(\omega) &= \sum_{\ell=1}^N c_{\ell\alpha}^* c_{\ell\nu} \frac{J_\ell(\omega)}{2}, \quad F_{\alpha\nu}(\omega) = \sum_{\ell=1}^N c_{\ell\alpha}^* c_{\ell\nu} \frac{J_\ell(\omega) n_\ell(\omega)}{2}. \end{aligned} \quad (7)$$

Here the integration over  $\omega$  is over all bath energy levels. Also we have taken observation times  $t \gg \tau_B$ , where  $\tau_B$  is the characteristic relaxation time scale of the bath. For baths with wide bandwidth and at low temperature,  $\tau_B \sim \beta$  (see the Appendix). A similar RQME was derived in Refs. [30,31] for slightly different systems.

### C. Equations for correlation functions

We note that it is possible to obtain closed time-dependent equations for the full set of two-point correlations  $C_{\alpha\nu}(t) = \text{Tr}[\rho(t) \hat{A}_\alpha^\dagger \hat{A}_\nu]$ . The evolution equation for  $C_{\alpha\nu}(t)$  as obtained from the QME is

$$\begin{aligned} \frac{dC_{\alpha\nu}}{dt} &= i\omega_\alpha C_{\alpha\nu}(t) + \varepsilon^2 \left[ F_{\nu\alpha}(\omega_\alpha) + iF_{\nu\alpha}^\Delta(\omega_\alpha) \right. \\ &\quad \left. - \sum_{\sigma=1}^N C_{\alpha\sigma}(t) v_{\nu\sigma} \right] + (\alpha \leftrightarrow \nu)^\dagger, \\ v_{\alpha\nu} &= f_{\alpha\nu}(\omega_\nu) + i f_{\alpha\nu}^\Delta(\omega_\nu), \end{aligned} \quad (8)$$

with  $f_{\alpha\nu}^\Delta(\omega) = \mathcal{P} \int \frac{d\omega' f_{\alpha\nu}(\omega')}{\pi(\omega - \omega')}$ ,  $F_{\alpha\nu}^\Delta(\omega) = \mathcal{P} \int \frac{d\omega' F_{\alpha\nu}(\omega')}{\pi(\omega - \omega')}$ , where  $\mathcal{P}$  denotes principal value.

The Redfield equation is, in general, quite difficult to solve. That is one of the main reasons for reduction of the Redfield equation to Lindblad forms, for which various numerical techniques are available. However, note that Eq. (8) forms a closed set of linear differential equations which can be easily solved numerically. Various physical quantities of interest such as occupation density and particle current can be obtained from these correlation functions. The main prerequisite for solving Eq. (8) is diagonalization of the system Hamiltonian to go to the eigenbasis. For a noninteracting bosonic or fermionic system of  $N$  sites in arbitrary lattices, this only requires diagonalization of the  $N \times N$  matrix  $H^{(S)}$ . If there are no further symmetries in the system, one needs all the  $N^2$  two-point correlation functions to close the set of linear differential equations and hence needs to deal with  $N^2 \times N^2$  matrices. Thus, Eq. (8) gives a numerical way to directly calculate time dynamics of out-of-equilibrium two-point correlation functions in an arbitrary system of noninteracting particles in a lattice. In the rest of the paper we will test the validity of solutions of Eq. (8).

### III. $N = 2$ CASE: COMPARISON BETWEEN QME AND EXACT RESULTS

The solution of Eq. (8) gives two-point correlation functions for the  $N$ -site noninteracting bosons or fermions in nonequilibrium in any dimension. We propose checking the validity of such solutions. To do so, we now go to a specific simple problem with  $N = 2$  sites and check how well Eq. (8) does when compared to exact results.

We consider the following specific two-site system coupled to baths which are one-dimensional chains:

$$\begin{aligned} \hat{\mathcal{H}}_S &= \omega_0(\hat{a}_1^\dagger \hat{a}_1 + \hat{a}_2^\dagger \hat{a}_2) + g(\hat{a}_1^\dagger \hat{a}_2 + \hat{a}_2^\dagger \hat{a}_1), \\ \hat{\mathcal{H}}_B^{(\ell)} &= t_B \left( \sum_{s=1}^{\infty} \hat{b}_s^{\ell\dagger} \hat{b}_{s+1}^\ell + \text{H.c.} \right), \quad \hat{\mathcal{H}}_B = \hat{\mathcal{H}}_B^{(1)} + \hat{\mathcal{H}}_B^{(2)}, \quad (9) \\ \hat{\mathcal{H}}_{SB} &= \varepsilon\gamma_1(\hat{a}_1^\dagger \hat{b}_1^1 + \text{H.c.}) + \varepsilon\gamma_2(\hat{a}_2^\dagger \hat{b}_1^2 + \text{H.c.}), \end{aligned}$$

where the operators are either all bosonic or all fermionic and  $\hat{b}_s^\ell$  is the annihilation operator of the  $s$ th bath site of the  $\ell$ th bath. The eigenmodes of the system are given by  $\hat{A}_1 = (\hat{a}_1 - \hat{a}_2)/\sqrt{2}$ ,  $\hat{A}_2 = (\hat{a}_1 + \hat{a}_2)/\sqrt{2}$ , with eigenvalues  $\omega_1 = \omega_0 - g$ ,  $\omega_2 = \omega_0 + g$ . We assume  $\omega_0 \gg \varepsilon$ , so that QME can be applied, while the parameter  $g$  can be varied freely. The bath spectral functions, defined in Eq. (3), can be obtained explicitly by going to eigenmodes of the baths and are given by [46] (see the Appendix)

$$J_\ell(\omega) = \frac{2\gamma_\ell^2}{t_B} \sqrt{1 - \left( \frac{\omega}{2t_B} \right)^2}. \quad (10)$$

In the following sections we first give some details of the exact approaches to obtain the steady state (Sec. III A) and time dynamics (Sec. III B) and then present some analytic results from RQME (Sec. III C), discuss the reduction to the Lindblad form (Sec. III D), and, finally, present the comparisons between the various methods (Sec. III E).

#### A. Exact results: Steady state via the quantum Langevin Equation (QLE)

Exact steady-state properties of the system can be found using QLE, as done in Refs. [44–46]. We briefly outline the procedure for computing physical quantities from the QLE method for the two-site case with the Hamiltonian given by Eq. (9). We first go to the eigenmodes of the bath by doing a unitary transformation. So  $\hat{\mathcal{H}}_B^{(\ell)} = t_B(\sum_{s=1}^{\infty} \hat{b}_s^{\ell\dagger} \hat{b}_{s+1}^\ell + \text{H.c.}) = \sum_{r=1}^{\infty} \Omega_r^\ell \hat{B}_r^{\ell\dagger} \hat{B}_r^\ell$ , where  $\hat{b}_s^\ell = \sum_r U_{rs}^{\ell*} \hat{B}_r^\ell$  and  $U$  is a unitary matrix that diagonalizes  $\hat{\mathcal{H}}_B^{(\ell)}$ .  $\hat{B}_r^\ell$  is the annihilation operator

of the eigenmode with eigenvalue  $\Omega_r^\ell$ . The bath eigenmodes satisfy the initial bath correlation functions:  $\langle \hat{B}_r^\ell \rangle = 0$  and  $\langle \hat{B}_r^\ell \hat{B}_s^\ell \rangle = n_\ell(\Omega_r^\ell) \delta_{rs}$ . We then have  $\kappa_{\ell r} = \gamma_\ell U_{r1}^{\ell*}$ . The EOMs for the system and the bath are

$$\frac{d\hat{B}_r^\ell}{dt} = -i[\hat{B}_r^\ell, \hat{\mathcal{H}}] = -i(\Omega_r^\ell \hat{B}_r^\ell + \varepsilon \kappa_{\ell r}^* \hat{a}_\ell), \quad (11)$$

$$\frac{d\hat{a}_1}{dt} = -i\left(\omega_0 \hat{a}_1 + g \hat{a}_2 + \sum_r \varepsilon \kappa_{1r} \hat{B}_r^{(1)}\right), \quad (1 \leftrightarrow 2). \quad (12)$$

The equation for the bath [Eq. (11)] can be formally solved to obtain

$$\hat{B}_r^\ell(t) = \hat{B}_r^\ell(0) e^{-i\Omega_r^\ell t} - i \varepsilon \kappa_{\ell r}^* \int_0^t dt' \hat{a}_\ell(t') e^{-i\Omega_r^\ell(t-t')}. \quad (13)$$

Using this in Eq. (12), we obtain the QLE,

$$\frac{d\hat{a}_1}{dt} = -i(\omega_0 \hat{a}_1 + g \hat{a}_2) - i \varepsilon \hat{\xi}_1 - \varepsilon^2 \int_0^t dt' \hat{a}_1(t') \alpha_1(t-t') \quad (1 \leftrightarrow 2), \quad (14)$$

where

$$\hat{\xi}_\ell(t) = \sum_r \kappa_{\ell r} \hat{B}_r^\ell(0) e^{-i\Omega_r^\ell t}, \quad (15)$$

$$\alpha_\ell(t-t') = \int \frac{d\omega}{2\pi} J_\ell(\omega) e^{-i\omega(t-t')} \quad (16)$$

represent ‘‘noise’’ and ‘‘dissipation,’’ respectively and  $J_\ell(\omega)$  are the bath spectral functions as defined in Eq. (3). Using the bath correlations, we obtain

$$\langle \hat{\xi}_\ell^\dagger(t') \hat{\xi}_\ell(t) \rangle = \int \frac{d\omega}{2\pi} J_\ell(\omega) n_\ell(\omega) e^{-i\omega(t-t')}. \quad (17)$$

Note that even though Eq. (14) has the form of a generalized Langevin equation, it is completely exact. The noise and dissipation that appear in the QLE arise from exact treatment of the bath. The steady-state results can be easily found from Eq. (14) by taking  $t \rightarrow \infty$  and doing Fourier transforms. The NESS current and occupation obtained are given by

$$I = g^2 \varepsilon^2 \int \frac{d\omega}{2\pi} \frac{J_1(\omega) J_2(\omega) [n_1(\omega) - n_2(\omega)]}{|\mathcal{M}(\omega)|^2}, \quad (18)$$

$$\langle \hat{a}_1^\dagger \hat{a}_1 \rangle = \varepsilon \int \frac{d\omega}{2\pi} \left[ \frac{\mathcal{K}(\omega) J_1(\omega) n_1(\omega)}{|\mathcal{M}(\omega)|^2} + \frac{g^2 J_2(\omega) n_2(\omega)}{|\mathcal{M}(\omega)|^2} \right], \quad (19)$$

where

$$\begin{aligned} \Delta_\ell(\omega) &= \mathcal{P} \int \frac{d\omega'}{2\pi} \frac{J_\ell(\omega')}{\omega - \omega'}, \\ \mathcal{M}(\omega) &= \left[ \left( \omega_0 - \omega - i\varepsilon^2 \frac{J_1(\omega)}{2} + \varepsilon^2 \Delta_1(\omega) \right) \right. \\ &\quad \left. \times \left( \omega_0 - \omega - i\varepsilon^2 \frac{J_2(\omega)}{2} + \varepsilon^2 \Delta_2(\omega) \right) - g^2 \right], \\ \mathcal{K}(\omega) &= \left| \omega_0 - \omega - i\varepsilon^2 \frac{J_2(\omega)}{2} + \varepsilon^2 \Delta_2(\omega) \right|^2. \end{aligned} \quad (20)$$

The occupation of the second site is just  $\langle \hat{a}_2^\dagger \hat{a}_2 \rangle = 1 \leftrightarrow 2$  in Eq. (19). All integrals over  $\omega$  go over all possible values

of  $\omega$ . Note that Eqs. (18) and (19) are exact results without any approximation. However, they are not closed-form results and involve some complicated integrals. Also, obtaining exact transient behavior using this method is difficult. But transient behavior can be easily obtained by exact numerics.

## B. Exact results: Time dynamics via system-bath numerics

To check the time dynamics we do numerical simulations. For this purpose, we choose a bath of finite size and evolve the full system-bath Hamiltonian  $\hat{\mathcal{H}}$  using unitary Hamiltonian dynamics. Let us collectively denote by  $d$  a column vector with all annihilation operators of both system and baths. The full Hamiltonian can be written as  $\hat{\mathcal{H}} = \sum_{i,j} H_{ij} d_i^\dagger d_j$ , where  $i$  now refers to either system or bath sites. If  $D = \langle dd^\dagger \rangle$  denotes the full correlation matrix of system and baths, its time evolution is given by  $D(t) = e^{iHt} D e^{-iHt}$ . In our simulations we considered the system described by Eq. (9) of two sites connected to baths each with 511 sites, which are large enough to show negligible finite-size effects.

## C. Correlation functions from RQME

### 1. Symmetric coupling to baths: $\gamma_1 = \gamma_2$ , full solution

In Eq. (8), this corresponds to the special case of all system-bath couplings being equal, i.e., when  $J_\ell(\omega) = J(\omega)$ . Under this condition Eq. (8) can be solved exactly using the fact that  $f_{\nu\sigma}(\omega) = [J(\omega)/2] \sum_{r=1}^N c_{\ell\nu}^* c_{\ell\sigma} = [J(\omega)/2] \delta_{\nu\sigma}$  due to orthonormality of the eigenfunctions. Thus,  $v_{\nu\sigma} = 0 \forall \nu \neq \sigma$ . Then Eq. (8) admits the exact solution:

$$C_{\alpha\nu}(t) = C_{\alpha\nu}(0) e^{-w_{\alpha\nu} t} + \varepsilon^2 \frac{u_{\alpha\nu}^* + u_{\nu\alpha}}{w_{\alpha\nu}} (1 - e^{-w_{\alpha\nu} t}), \quad (21)$$

where  $w_{\alpha\nu} = -i\omega_\alpha + \varepsilon^2 [if_{\alpha\alpha}^\Delta(\omega_\alpha) + f_{\alpha\alpha}(\omega_\alpha)] + (\alpha \rightarrow \nu)^*$  and  $u_{\nu\alpha} = F_{\nu\alpha}(\omega_\alpha) + iF_{\nu\alpha}^\Delta(\omega_\alpha)$ . Note that the baths can still be at different temperatures and chemical potentials. So in this case, we have full time-dependent analytical closed-form results for out-of-equilibrium correlation functions that hold for all values of  $g$ .

### 2. Asymmetric couplings to baths: $\gamma_1 \neq \gamma_2$ , $g \gg \frac{\varepsilon^2}{t_B}$

Closed-form analytical results are difficult to obtain for all  $g$  when  $\gamma_1 \neq \gamma_2$ . But for  $g \gg \frac{\varepsilon^2}{t_B}$ , the analytical closed form for time dynamics can be found by solving Eq. (8) perturbatively up to leading order in  $\varepsilon$ . The results are

$$N_\alpha(t) \simeq N_\alpha(0) e^{-2\varepsilon^2 f_{\alpha\alpha}(\omega_\alpha) t} + \frac{F_{\alpha\alpha}(\omega_\alpha)}{f_{\alpha\alpha}(\omega_\alpha)} (1 - e^{-2\varepsilon^2 f_{\alpha\alpha}(\omega_\alpha) t}), \quad (22a)$$

$$\begin{aligned} C_{12}(t) &\simeq C_{12}(0) e^{-w_{12} t} + \frac{i\varepsilon^2}{g} \{ [F_{12}(\omega_2) - iF_{12}^\Delta(\omega_2)] \\ &\quad \times (1 - e^{-w_{12} t}) + v_{21} [N_1(0) e^{-w_{12} t} - N_1(t)] \\ &\quad + (1 \leftrightarrow 2)^* \}, \end{aligned} \quad (22b)$$

where  $N_\alpha(t) = C_{\alpha\alpha}(t)$  and  $w_{12} = -i\omega_1 + \varepsilon^2 [if_{11}^\Delta(\omega_1) + f_{11}(\omega_1)] + (1 \rightarrow 2)^*$ .

Note that since we have already assumed  $t \gg \tau_B$ , the transient dynamics given by the above equations can only

be trusted if the relaxation time of the system is much larger than  $\tau_B$ , viz.,  $\tau_B \ll 1/[\varepsilon^2 f_{\alpha\alpha}(\omega_\alpha)] \sim \frac{t_B}{\varepsilon^2}$ , since  $f_{\alpha\alpha}(\omega_\alpha) \sim t_B$ , from Eqs. (10) and (7). Since  $f_{\alpha\alpha}(\omega_\alpha) > 0$ , it can be seen from Eqs. (21), (22a), and (22b) that the correlation functions approach steady-state values at time  $t \gg 1/[\varepsilon^2 f_{\alpha\alpha}(\omega_\alpha)] \sim \frac{t_B}{\varepsilon^2}$ , and the steady-state values are independent of the initial state. So we can easily get steady-state values of mode occupation  $N_\alpha^{ss}$  and current between the first and second sites,  $I_{1 \rightarrow 2} = -g i \langle \hat{a}_1^\dagger \hat{a}_2 - \hat{a}_2^\dagger \hat{a}_1 \rangle = g i \langle \hat{A}_1^\dagger \hat{A}_2 - \hat{A}_2^\dagger \hat{A}_1 \rangle = 2g \text{Im}(C_{12})$ :

$$N_\alpha^{ss} \simeq \frac{J_1(\omega_\alpha)n_1(\omega_\alpha) + J_2(\omega_\alpha)n_2(\omega_\alpha)}{J_1(\omega_\alpha) + J_2(\omega_\alpha)}, \quad (23a)$$

$$I_{1 \rightarrow 2} \simeq \frac{\varepsilon^2}{2} \sum_{\alpha=1}^2 \frac{J_1(\omega_\alpha)J_2(\omega_\alpha)[n_1(\omega_\alpha) - n_2(\omega_\alpha)]}{J_1(\omega_\alpha) + J_2(\omega_\alpha)}. \quad (23b)$$

It is seen from the steady-state equations that in equilibrium, i.e., when  $n_1(\omega) = n_2(\omega) = n(\omega)$ ,  $N_\alpha = n(\omega)$  and current is zero, which are the expected thermal values. Thus, RQME shows proper thermalization and approaches to steady state.

#### D. Reduction to the Lindblad form

The RQME is not in the Lindblad form. But it can be reduced to the Lindblad form by making certain further approximations. There are two popular forms of the Lindblad equations using either the local operators  $a_\ell$  or the eigenbasis operators  $A_\nu$  [Eq. (6)]. We briefly discuss how they are obtained and their expected regimes of validity.

##### 1. Local Lindblad QME (LLQME) ( $g < \varepsilon$ )

The local Lindblad equation for this system has the form  $\partial\rho/\partial t = i[\rho, \hat{\mathcal{H}}_S] + \varepsilon^2(\mathcal{L}_1^{LL}\rho + \mathcal{L}_2^{LL}\rho)$ , where

$$\begin{aligned} \mathcal{L}_\ell^{LL}\rho = & J(\omega_0)e^{\beta\varepsilon(\omega_0 - \mu\varepsilon)}n(\omega_0)\left(\hat{a}_\ell\rho\hat{a}_\ell^\dagger - \frac{1}{2}\{\hat{a}_\ell^\dagger\hat{a}_\ell, \rho\}\right) \\ & + J(\omega_0)n(\omega_0)\left(\hat{a}_\ell^\dagger\rho\hat{a}_\ell - \frac{1}{2}\{\hat{a}_\ell\hat{a}_\ell^\dagger, \rho\}\right). \end{aligned} \quad (24)$$

For  $g < \varepsilon$ , RQME [Eq. (7)] can be reduced to LLQME by expanding the nonunitary dissipative part about  $g = 0$  and keeping the first term. This is because the dissipative part is already  $O(\varepsilon^2)$ , and since  $g < \varepsilon$ , higher-order terms in  $g$  will give higher-order terms in  $\varepsilon$ , which we neglect in the RQME treatment. This amounts to putting  $\omega_\nu = \omega_0$  in the dissipative part of Eq. (7). The same result is more conventionally obtained by considering the intersite hopping term in the system Hamiltonian to be small and treating it as a part of the system-bath Hamiltonian while deriving the QME. This directly leads to the LLQME. Thus, LLQME is valid when  $g < \varepsilon$ . LLQME results for current and occupation for this problem have been derived in previous papers [24,25]. The equilibrium condition  $N_\alpha = n(\omega)$  is not obtained from LLQME since, for  $g < \varepsilon$ , each site interacts with its bath more strongly than with the other site, thereby thermalizing with its own bath. It clearly follows that if there were only one site, it would show thermalization. Thus, the regime of validity of LLQME is too restrictive to show thermalization for a system with more than one noninteracting degree of freedom.

However, in interacting systems, it has recently been shown that even LLQME is capable of showing thermalization [49].

##### 2. Eigenbasis Lindblad QME (ELQME) ( $g \gg \frac{\varepsilon^2}{t_B}, C_{12}^{ss} = 0$ )

The eigenbasis Lindblad equation for this system has the form  $\frac{\partial\rho}{\partial t} = i[\rho, \hat{\mathcal{H}}_S] + \varepsilon^2(\mathcal{L}_1^{EL}\rho + \mathcal{L}_2^{EL}\rho)$ , where

$$\begin{aligned} \mathcal{L}_\alpha^{EL}\rho = & [f_{\alpha\alpha}(\omega_\alpha) \mp F_{\alpha\alpha}(\omega_\alpha)](2\hat{A}_\alpha\rho\hat{A}_\alpha^\dagger - \{\hat{A}_\alpha^\dagger\hat{A}_\alpha, \rho\}) \\ & + F_{\alpha\alpha}(\omega_\alpha)(2\hat{A}_\alpha^\dagger\rho\hat{A}_\alpha - \{\hat{A}_\alpha\hat{A}_\alpha^\dagger, \rho\}). \end{aligned} \quad (25)$$

Equation (7) is reduced to ELQME under rotating-wave or secular approximation [50,51], which amounts to neglecting  $\alpha \neq \nu$  terms in the sum in Eq. (7). The rotating-wave approximation assumes that the observation time  $t \gg \frac{1}{g}$ . On the other hand, to give the correct steady state, the QME must be valid for times shorter than the time needed to reach steady state. This means that we need the QME to be valid at times  $t \lesssim \frac{t_B}{\varepsilon^2}$  since we have already seen that the time required to reach steady state  $\sim \frac{t_B}{\varepsilon^2}$ . The two conditions are valid together if  $g \gg \frac{\varepsilon^2}{t_B}$ . This seems like a rather weak condition.

However, we note that, while these are the necessary conditions for obtaining ELQME, there is no guarantee that the resulting ELQME will reproduce all physical observables accurately. In particular, neglecting  $\alpha \neq \nu$  terms in the sum in Eq. (7) means ELQME has no terms connecting  $\hat{A}_1$  and  $\hat{A}_2$ . Therefore, it gives  $C_{12}^{ss} = 0$ , where  $C_{12}^{ss}$  is the steady-state value of  $C_{12}$ . This condition is, of course, valid only in equilibrium, where there is no current. Thus, although the rotating-wave or secular approximation is a good approximation for equilibrium properties, it is a bad approximation in nonequilibrium. This point has also been succinctly discussed in a recent work [29].

However, ELQME still can be used to correctly obtain some nonequilibrium results. For example, for  $g \gg \frac{\varepsilon^2}{t_B}$  ELQME gives the same equation for  $N_\alpha$  as Eqs. (22a) and (23a). This result then can be used to obtain the correct current between the left bath and the system [18,28]. Thus, ELQME suffers from a drawback that one is only able to compute the net current flowing between the two reservoirs in the NESS but not the current distributions in the system (e.g., current flowing along two arms in a ring geometry). This also indicates a physical inconsistency of the ELQME formalism in nonequilibrium (see the Appendix).

#### E. Comparison of results from various methods and discussions

Finally, we now present a detailed comparison of results obtained using the various approaches for both steady-state and time-dependent properties. For the two-site problem we consider the bosonic and fermionic versions and compute quantities such as the occupation number and particle current from site 1 to site 2. We again summarize the various approaches that we use:

(i) For steady-state properties, these are exactly computed using Eqs. (18) and (19) following the QLE approach.

(ii) Exact time-dependent properties are obtained from the numerical approach discussed in Sec. III B.

(iii) The equations for correlation functions, Eqs. (8), are solved to obtain the predictions of RQME. We also evaluate the perturbative solution of these equations given in Eqs. (22a) and (22b).

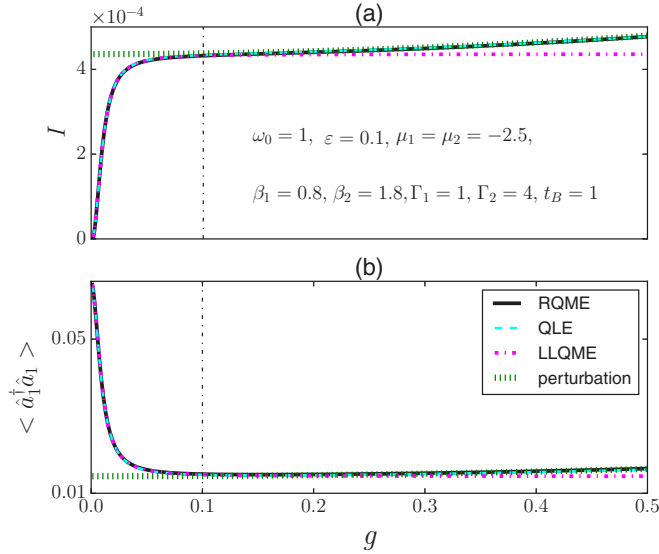


FIG. 2. Bosonic model: steady-state properties. (a) Particle current and (b) the occupation number in the left site as a function of intersite hopping  $g$  for the two-site boson problem. RQME shows near perfect agreement with exact results from QLE for all values of  $g$ , while LLQME and perturbation results [Eqs. (23a) and (23b)] are valid in their respective limits. The vertical line marks the position of  $g = \varepsilon$ , below which LLQME is valid. The parameter  $\Gamma_{1,2} = 2\gamma_{1,2}^2/t_B$  is related to the system-bath coupling [see Eq. (10)]. Current is measured in units of  $\omega_0$ , and all energy variables are measured in units of  $\hbar\omega_0$ .

(iv) One can also write the equations for two-point correlations obtained from the Lindblad approach, and these are solved to obtain the predictions from LLQME.

(v) The ELQME approach cannot directly give the current inside the system. The predictions for the occupation number are the same as those from the perturbative solution of Eq. (22a).

We emphasize that all the approaches that we discuss are based on the same starting microscopic model of a system and baths, given by Eqs. (9), which leads to the bath spectral function, Eq. (10).

For the bosonic case, the steady-state results for current and occupation number are shown in Fig. 2, and results for time dynamics are shown in Figs. 3 and 4. For the time dynamics, for the results presented here, the initial condition corresponds to no particles inside the system and baths in equilibrium at different  $\mu$  and  $T$ . But we have tested other initial conditions like a finite number of particles in the system and random initial values of the correlation functions. The following observations are true for such generic initial conditions for the system. For the fermionic case, the results for the steady-state current as a function of voltage difference and of the intrasystem coupling  $g$  are shown in Fig. 5. In all cases, the system-bath coupling is chosen to be asymmetric, i.e.,  $\gamma_1 \neq \gamma_2$ .

Our most important observation is that RQME results obtained from the solution of Eq. (8) agree very well with exact results from QLE and numerics for all values of  $g$  for steady state, as well as for long-time dynamics. LLQME agrees well for  $g < \varepsilon$ , as expected. In Fig. 3, we show that the

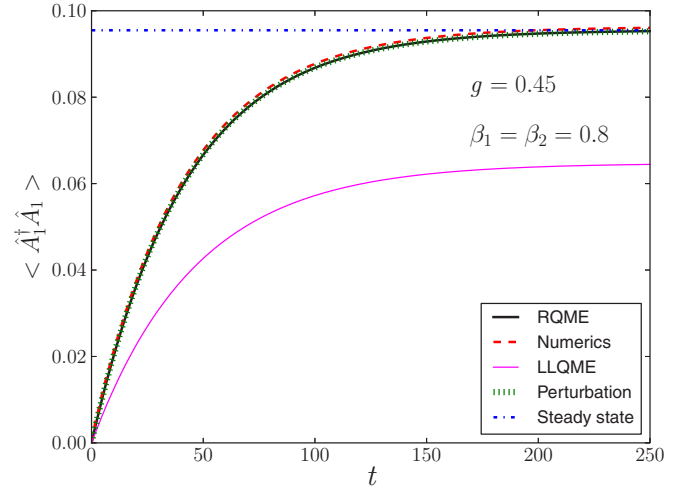


FIG. 3. Bosonic model: thermalization. We show the time evolution of occupation of the lower-energy mode  $\hat{A}_1$ , corresponding to energy  $\omega_1 = \omega_0 - g$ , in equilibrium for the two-site boson problem, starting from an empty system, for  $g = 0.45$ . The steady state (horizontal line) corresponds to the value of Bose distribution  $n(\omega_1) = [e^{\beta(\omega_1 - \mu)} - 1]^{-1}$  with the equilibrium bath temperatures and chemical potentials. LLQME does not show thermalization because it is not valid for  $g > \varepsilon$ , while exact numerical results, RQME results, and the perturbation result [Eqs. (22a)] match and show thermalization. All parameters not explicitly specified are the same as in Fig. (2). Current is measured in units of  $\omega_0$ , and all energy variables are measured in units of  $\hbar\omega_0$ . Time is measured in units of  $\omega_0^{-1}$ .

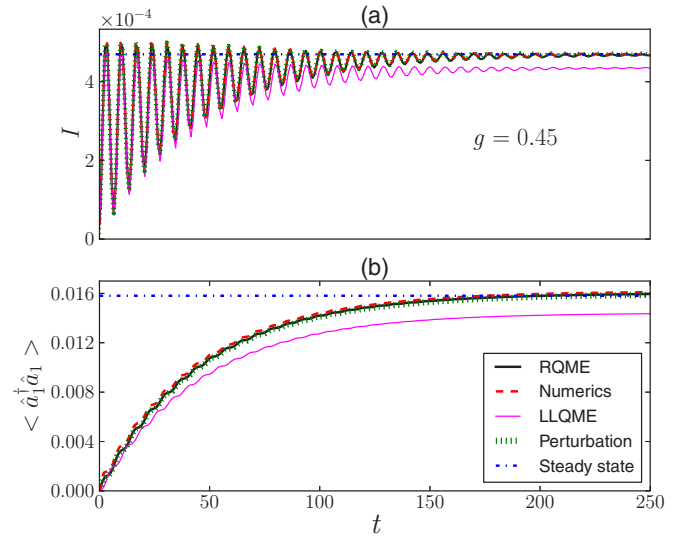


FIG. 4. Bosonic model: nonequilibrium time dynamics. We show the time evolution of (a) particle current and (b) occupation number of the left site for the two-site boson problem, starting from an empty system, for  $g = 0.45$ . RQME results show good agreement with exact numerics. Since  $g > \varepsilon$ , LLQME does not match, while the perturbation result [Eqs. (22a) and (22b)] matches with RQME. The horizontal line shows the exact steady-state result obtained from QLE. All parameters not explicitly specified are the same as in Fig. (2). Current is measured in units of  $\omega_0$ , and all energy variables are measured in units of  $\hbar\omega_0$ . Time is measured in units of  $\omega_0^{-1}$ .

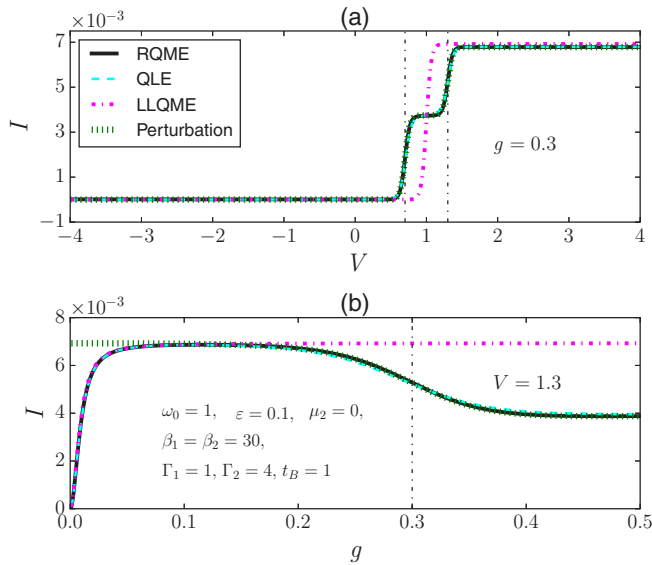


FIG. 5. Fermionic model: steady-state properties. (a) Particle current vs voltage and (b) particle current vs intersite hopping in the two-site fermion problem. The vertical lines correspond to positions where potential difference  $V = \mu_1 - \mu_2 = \omega_\alpha$ , where  $\omega_\alpha$  are the system energy levels. RQME shows nearly perfect agreement with exact results from QLE for all values of  $g$ , while LLQME and perturbation results [Eqs. (23a) and (23b)] are valid in their respective limits. The graphs demonstrate the effect of conductance quantization at low temperatures. The parameter  $\Gamma_{1,2} = 2\gamma_{1,2}^2/t_B$ . Current is measured in units of  $\omega_0$ , and all energy variables are measured in units of  $\hbar\omega_0$ .

system indeed thermalizes in equilibrium, and this is perfectly captured by RQME and not by LLQME since it is invalid for  $g > \varepsilon$ . For  $g \gg \frac{\varepsilon^2}{t_B}$ , our analytical closed-form perturbation results match quite well with the exact results, showing the correct approach to steady state and thermalization. Therefore, we conclude that RQME gives the correct physics under the Born-Markov approximation.

Apart from validating the RQME description, we also observe interesting physical trends. The boson problem may be realized in bosonic cold-atom experiments or in optical cavity experiments with a suitable choice of parameters and spectral functions. We see in Fig. 2 that steady-state properties have a markedly different behavior depending on whether  $g < \varepsilon$  or  $g > \varepsilon$ . For  $g < \varepsilon$ , the current increases rapidly, but after that there is a slow increase in current. Also, for  $g < \varepsilon$  the occupation of the left cavity becomes minimum when  $g \simeq \varepsilon$ . However, beyond this point, the occupation of the left cavity increases slowly with an increase in tunneling probability  $g$ . These trends may be experimentally observed. However, these trends depend on the choice of the bath spectral function  $J_\ell(\omega)$ . For example, for optical cavity experiments, the commonly used Ohmic dissipation  $J_\ell(\omega) \propto \omega$  will give a slow decrease of current with  $g$  for  $g > \varepsilon$ , still showing a markedly different behavior from the  $g < \varepsilon$  case. Here we microscopically derived  $J_\ell(\omega)$  assuming a microscopic model of the bath.

The fermionic system of two sites may be experimentally realized in noninteracting quantum dots or in fermionic cold-

atom experiments. The current versus voltage plot of the fermionic system shows the effect of conductance quantization, which is observed experimentally [13]. The current versus hopping  $g$  plot shows suppression of current after a value of  $g$ . These observations can be explained as follows. The two-site system has two eigenenergy levels of energy  $\omega_0 - g$  and  $\omega_0 + g$ . In Fig. 5, the right bath is held at zero chemical potential while the chemical potential of the left bath,  $\mu_1$ , is varied. When  $\mu_1 \ll \omega_0 - g$ , no fermion from the left bath has the energy to enter the system. So there is no flow of current. When  $\omega_0 - g \ll \mu_1 \ll \omega_0 + g$ , the fermions can hop through the system via the lower-energy level. So a finite current flows through the system. When  $\mu_1 \gg \omega_0 + g$ , fermion transport through the system can occur through both energy levels. Since all system levels are now participating in transport, increasing  $\mu_1$  beyond this point does not affect current any more. For a similar reason, suppression of current occurs when  $g \gg \mu_1 - \omega_0$  in the current versus  $g$  plot. These observations can also be easily obtained for larger systems.

The NESS for the fermionic problem was solved earlier by a RQME method but in the limit of negligible Fock space coherences [36], which gives results identical to the  $g \gg \frac{\varepsilon^2}{t_B}$  results [Eqs. (23a) and (23b)]. However, their method of solution [36] cannot easily be generalized to treat the bosonic version of the problem.

One important issue with the Redfield operator is that it is not completely positive. In a recent work [40], it was shown to lead to negative entropy production in a specific system. In this paper we find RQME to give the correct Born-Markov approximated results for correlation functions (closely related to physical observables), both equilibrium and time dynamics. But the situation regarding nonpositivity of the Redfield operator is not completely clear and requires further investigation.

#### IV. CONCLUSIONS

Quantum master equations derived under the Born-Markov approximation are widely used to describe open quantum systems. But the validity of such approximate QMEs has not been, to our knowledge, rigorously checked before. In this work, by studying a simple system of noninteracting bosons or fermions and comparing results from the microscopically derived Redfield QME under the Born-Markov approximation with exact results, we showed that the Redfield QME indeed gives very accurate results in a wide parameter range. Moreover, we observe that, rotating-wave or secular approximations that are often done to reduce the Redfield QME to the eigenbasis Lindblad form are inappropriate in a nonequilibrium setting. On the other hand, the small hopping approximation that is often employed to reduce the Redfield QME to the local Lindblad form is very restrictive for noninteracting particles. These observations are consistent with previous results [27–29]. So one is required to work with the full Redfield QME to obtain the correct physics in a nonequilibrium system of noninteracting bosons or fermions.

One of the reasons a Redfield equation is often reduced to the Lindblad form is easy numerical treatment. The Redfield equation is, in general, much more difficult to solve than the Lindblad equations. However, for the case of noninteracting

bosons or fermions in an arbitrary lattice in any dimension, here we presented a complete set of linear differential equations [Eq. (8)] for two-point correlation functions which can be easily solved numerically. Equation (8) therefore gives a numerical way to directly calculate the time dynamics of out-of-equilibrium two-point correlation functions in an arbitrary system of noninteracting particles in a lattice. Various physical observables can be directly calculated from such correlation functions.

For a two-site system we derived closed-form analytical expressions for out-of-equilibrium time dynamics of two-point correlation functions [Eqs. (21), (22a), and (22b)]. These analytical results explicitly show that the correlation functions approach a steady-state value independent of initial conditions, and these steady-state values give the expected thermalization in equilibrium. They also match the numerically obtained exact results from other methods independent of any approximate master equation, thereby validating the Redfield approach. Various physical quantities like site occupation and current calculated from the correlation functions show interesting experimentally observable trends which are seen in parameter regimes beyond the regime of validity of Lindblad methods. These trends may be seen in experiments with cavity QED, cold atoms, quantum dots, etc. Needless to say, recent cutting-edge technologies can be exploited to engineer Hamiltonians and reservoirs such that the discrepancy between Lindblad methods and exact results can be made visible.

The nonpositivity of the Redfield operator remains an important issue and needs further work. However, this does not seem to be a problem in reproducing correct physical steady-state properties and correct long-time dynamics in our system.

We reemphasize that the main conclusion of our present work is that it is, indeed, justified to adopt RQME in order to go beyond the limitations of the Lindblad methods. Future work involves RQME with similar rigorous treatment of reservoirs for open quantum non-linear (interacting) systems where exact methods are not available, for e.g., Jaynes–Cummings, spin boson, open  $XY$  spin chains, Dicke type models [6,9,52–61]. Such a RQME approach could unravel interesting out-of-equilibrium many-body phenomena that may be missed by conventional Lindblad-type approaches.

#### ACKNOWLEDGMENTS

We acknowledge fruitful discussions with R. Vijay, Y. Dubi, K. Saito, M. Esposito, J. L. Lebowitz, D. Huse, and H. Spohn. M.K. gratefully acknowledges support from the Professional Staff Congress of the City University of New York Award No. 68193-0046. A.D. acknowledges support from Indo-Israel joint research project F.No. 6-8/2014(IC). We are thankful for the hospitality of the Raman Research Institute and the International Centre for Theoretical Sciences of the Tata Institute of Fundamental Research, Bengaluru, during the workshop on statistical physics where several interesting discussions took place. We would also like to thank the International Centre for Theoretical Sciences of the Tata Institute of Fundamental Research, Bengaluru, for the hospitality during the program “Non-equilibrium statistical physics”, where this work culminated.

## APPENDIX

### 1. Derivation of Redfield QME

Here, we briefly outline the steps involved in obtaining our QME [Eq. (7)] from Eq. (4). We first go to the eigenbasis of the system through the transformation:  $\hat{a}_\ell = \sum_{\alpha=1}^N c_{\ell\alpha} \hat{A}_\alpha$ . Then to use Eq. (4), we need to go to the interaction picture representation,  $\hat{a}_\ell^I = \sum_{p=1}^N c_{\ell\alpha} \hat{A}_p e^{-i\omega_\alpha t}$ ,  $\hat{B}_r^{\ell I}(t) = \hat{B}_r^\ell e^{-i\Omega_r^\ell t}$ . Next, substituting into Eq. (4) and using the bath correlations [Eq. (2)] and bath spectral functions [Eq. (3)] and going back to Schrödinger picture, we obtain

$$\begin{aligned} \dot{\rho}(t) = & i[\rho, \hat{\mathcal{H}}_S] - \varepsilon^2 \sum_{\alpha, v, \ell=1}^N c_{\ell\alpha}^* c_{\ell v} \int_{\Omega_{\min}^\ell}^{\Omega_{\max}^\ell} \frac{d\omega}{2\pi} [ \{ [\rho(t) \hat{A}_v, \hat{A}_\alpha^\dagger] \\ & + [\hat{A}_\alpha^\dagger, \hat{A}_v \rho(t)] e^{\beta_\ell(\omega - \mu_\ell)} \} J_\ell(\omega) n_\ell(\omega) \int_0^t d\tau e^{i(\omega - \omega_v)\tau} \\ & + \text{H.c.}, \end{aligned} \quad (\text{A1})$$

where  $\Omega_{\min}^\ell, \Omega_{\max}^\ell$  are the minimum and the maximum energy levels of the bath coupled to the  $\ell$ th site. Now, assuming  $t \gg \tau_B$ , where  $\tau_B$  is the relaxation time scale of the bath, we replace the upper limit of the time integral in the above equation by  $t \rightarrow \infty$  to obtain our QME [Eq. (7)]. Even though this assumption is guaranteed to give the correct steady state, an estimate of  $\tau_B$  is required to ensure validity of the transient dynamics from our QME.  $\tau_B$ , of course, depends on the model of bath.

### 2. A bath model in the wideband limit

The model of the bath enters the calculation through the bath spectral function  $J_\ell(\omega) = 2\pi \sum_r |\kappa_{\ell r}|^2 \delta(\omega - \Omega_r^\ell)$ . Note that since in our derivation of RQME the system couples to the eigenmodes of the baths,  $\kappa_{\ell r}$  are proportional to the eigenfunctions of the bath Hamiltonian. Because of infinite degrees of freedom, the energy spectrum of the bath can be considered continuous. For our case of the Hamiltonian in Eq. (9), bath eigenenergies are  $\Omega(q_\ell) = -2t_B \cos q_\ell$  and  $\kappa(q_\ell) = \gamma_\ell \sqrt{\frac{2}{\pi}} \sin q_\ell$ , with  $0 \leq q_\ell \leq \pi$ . Thus,

$$\begin{aligned} J_\ell(\omega) = & 4\gamma_\ell^2 \int_0^\pi dq_\ell \sin^2 q_\ell \delta(\omega + 2t_B \cos q_\ell) \\ = & \frac{2\gamma_\ell^2}{t_B} \sqrt{1 - \frac{\omega^2}{4t_B^2}}. \end{aligned} \quad (\text{A2})$$

We also need the result  $\mathcal{P} \int \frac{d\omega' J_\ell(\omega')}{2\pi(\omega' - \omega)} = -\frac{\gamma_\ell^2 \omega}{2t_B^2}$  to calculate  $f_{\alpha v}^\Delta(\omega)$  [in Eq. (8)].  $F_{\alpha v}^\Delta(\omega)$  cannot be written in a simple closed form and is calculated numerically. The functions  $f_{\alpha v}(\omega), F_{\alpha v}(\omega)$  can be written down in matrix form as

$$f(\omega) = \frac{1}{4} \begin{bmatrix} J_1(\omega) + J_2(\omega) & J_1(\omega) - J_2(\omega) \\ J_1(\omega) - J_2(\omega) & J_1(\omega) + J_2(\omega) \end{bmatrix}, \quad (\text{A3})$$

$$F(\omega) = \frac{1}{4} \begin{bmatrix} J_1(\omega)n_1(\omega) + J_2(\omega)n_2(\omega) & J_1(\omega)n_1(\omega) - J_2(\omega)n_2(\omega) \\ J_1(\omega)n_1(\omega) - J_2(\omega)n_2(\omega) & J_1(\omega)n_1(\omega) + J_2(\omega)n_2(\omega) \end{bmatrix}, \quad (\text{A4})$$

### 3. Estimate of $\tau_B$

Now, for this bath model we estimate  $\tau_B$ . Looking at Eq. (A1), we find integrals of the type  $\mathcal{I}_1(\omega_\nu, t) = \int_0^t d\tau e^{-i\omega_\nu \tau} \mathcal{I}_2(\tau)$  with  $\mathcal{I}_2(\tau)$  given by

$$\mathcal{I}_2(\tau) = \int_{\Omega_{\min}^\ell}^{\Omega_{\max}^\ell} \frac{d\omega}{2\pi} J_\ell(\omega) n_\ell(\omega) e^{i\omega\tau}. \quad (\text{A5})$$

The time  $\tau_B^{(\ell)}$  at which  $\mathcal{I}_2(\tau)$  decays is the relaxation time of the  $\ell$ th bath. If the bandwidth of the bath is large enough,  $\mathcal{I}_2(\tau)$  is like a Fourier transform of  $J_\ell(\omega) n_\ell(\omega)$ , and hence,  $\tau_B^{(\ell)}$  depends on the spread of  $J_\ell(\omega) n_\ell(\omega)$ . At low temperatures the spread will be  $\sim 1/\beta_\ell$ . Hence,  $\tau_B^{(\ell)} \sim \beta_\ell$ .

As mentioned in the main text, the transient dynamics from our QME is valid only if the system relaxation time is much greater than  $\tau_B$ . From Eqs. (22a) and (22b), we see that system relaxation time is  $\sim \frac{1}{\varepsilon^2 f_{\alpha\alpha}(\omega_\alpha)}$ . Thus, for the validity of our transient dynamics,

$$\tau_B \ll \frac{1}{\varepsilon^2 f_{\alpha\alpha}(\omega_\alpha)} \quad \forall \alpha \in 1, 2, \dots, N. \quad (\text{A6})$$

For our two-site case,  $f_{\alpha\alpha}(\omega_\alpha) \sim t_B^{-1}$ . Thus, the condition for validity of transient dynamics for the two-site case becomes

$$\beta_\ell \ll \frac{t_B}{\varepsilon^2} \quad \forall \ell = 1, 2. \quad (\text{A7})$$

This condition is clearly satisfied by our choice of parameters.

### 4. Problem with ELQME

In the ELQME, problems arise in the definitions of NESS current. For our Hamiltonian (9), current can be derived from the following equations:

$$\frac{d\langle \hat{a}_1^\dagger \hat{a}_1 \rangle}{dt} = I_{B^{(1)} \rightarrow 1} - I_{1 \rightarrow 2}, \quad (\text{A8})$$

$$\frac{d\langle \hat{a}_1^\dagger \hat{a}_1 + \hat{a}_2^\dagger \hat{a}_2 \rangle}{dt} = I_{B^{(1)} \rightarrow 1} - I_{2 \rightarrow B^{(2)}}, \quad (\text{A9})$$

where  $I_{B^{(1)} \rightarrow 1}$  is the current between the left bath and the left system site,  $I_{1 \rightarrow 2}$  is the current between the left and right system sites, and  $I_{2 \rightarrow B^{(2)}}$  is the current between the right site and the right bath. Note that the expression for  $I_{1 \rightarrow 2}$  is the same for all three approaches (RQME, LLQME, ELQME) because it comes from the nondissipative part of the QME. On the

other hand, depending on whether the approach is RQME or LLQME or ELQME, the expressions for  $I_{B^{(1)} \rightarrow 1}$  and  $I_{2 \rightarrow B^{(2)}}$  are different as they come from the dissipative part. In NESS all three currents defined above are equal. This is true for RQME and LLQME. But ELQME gives  $I_{1 \rightarrow 2} = 0$  even in NESS while giving a nonzero current for  $I_{B^{(1)} \rightarrow 1}$ . In fact, Eq. (A8), from ELQME, becomes of the form  $\frac{d\langle \hat{a}_1^\dagger \hat{a}_1 \rangle}{dt} = I_{B^{(1)} \rightarrow 1} - I_{1 \rightarrow B^{(2)}}$ , where a fictitious  $I_{1 \rightarrow B^{(2)}}$  current from the left site to the right bath appears which is completely unphysical as there is no direct connection between the left site and the right bath. However, if Eq. (A9) is used, then ELQME gives the same result as that obtained from RQME in the limit  $g \gg (\varepsilon^2/t_B)$ . This is because  $I_{B^{(1)} \rightarrow 1}$  obtained from Eq. (A9) depends only on  $N_1, N_2$ , which are correctly given by ELQME when  $g \gg (\varepsilon^2/t_B)$ . Thus, although ELQME is not physically self-consistent, this trick can be used to obtain the correct current in our setup, as done in previous studies [18,28]. However, this trick will not work in cases with different geometries. For example, if two sites of a ring are connected to two different baths, ELQME will not be able to give current flowing in the two arms.

### 5. The Gibbs state

In equilibrium, the Gibbs state is defined as  $\rho_{\text{Gibbs}} = \frac{e^{-\beta(\hat{H}_S - \mu \hat{N}_S)}}{\text{Tr}(e^{-\beta(\hat{H}_S - \mu \hat{N}_S)})}$ , where  $\hat{N}_S = \sum_{\alpha=1}^N \hat{A}_\alpha^\dagger \hat{A}_\alpha$ . Note that, in contrast to what is often reported in the literature, the Gibbs state is not a stationary state of RQME [Eq. (7)] in equilibrium. This is because we do not neglect the principal-value terms  $f_{\alpha\nu}^\Delta(\omega)$  and  $F_{\alpha\nu}^\Delta(\omega)$  as is often done (for example, [34,36]). We find no reason to neglect them as the terms are not small and do not contribute to only shifting the system energy levels by a constant amount. For our two site Hamiltonian (9), for  $g \gg (\varepsilon^2/t_B)$ , the equilibrium steady state, which can be computed from the two point correlation functions, has  $O(\varepsilon^2)$  corrections over the Gibbs state. So, in this case, RQME gives the correct thermalization in the following sense:

$$\lim_{\varepsilon \rightarrow 0} \lim_{t \rightarrow \infty} \rho(t) = \rho_{\text{Gibbs}} \quad \forall \beta_1 = \beta_2 = \beta, \mu_1 = \mu_2 = \mu, \quad (\text{A10})$$

where the order of limits is important. ELQME, on the other hand, has the Gibbs state as its stationary state in equilibrium.

- [1] K. L. Hur, L. Henriët, A. Petrescu, K. Plekhanov, G. Roux, and M. Schiro, [arXiv:1505.00167](https://arxiv.org/abs/1505.00167).
- [2] A. A. Houck, H. E. Türeci, and J. Koch, *Nat. Phys.* **8**, 292 (2012).
- [3] D. L. Underwood, W. E. Shanks, J. Koch, and A. A. Houck, *Phys. Rev. A* **86**, 023837 (2012).

- [4] S. Schmidt and J. Koch, *Ann. Phys. (Berlin, Ger.)* **525**, 395 (2013)
- [5] K. Baumann, C. Guerlin, F. Brennecke, and T. Esslinger, *Nature (London)* **464**, 1301 (2010).
- [6] M. Kulkarni, B. Öztöp, and H. E. Türeci, *Phys. Rev. Lett.* **111**, 220408 (2013).

- [7] M. Aspelmeyer, T. J. Kippenberg, and F. Marquardt, *Rev. Mod. Phys.* **86**, 1391 (2014).
- [8] M. Ludwig and F. Marquardt, *Phys. Rev. Lett.* **111**, 073603 (2013).
- [9] M. Kulkarni, O. Cotlet, and H. E. Türeci, *Phys. Rev. B* **90**, 125402 (2014).
- [10] Y. Y. Liu, K. D. Petersson, J. Stehlik, J. M. Taylor, and J. R. Petta, *Phys. Rev. Lett.* **113**, 036801 (2014).
- [11] B. K. Agarwalla, M. Kulkarni, S. Mukamel, and D. Segal, [arXiv:1604.01811](https://arxiv.org/abs/1604.01811).
- [12] R. Härtle and M. Kulkarni, *Phys. Rev. B* **91**, 245429 (2015).
- [13] S. Krinner, D. Stadler, D. Husmann, J. Brantut, and T. Esslinger, *Nature (London)* **517**, 64 (2015).
- [14] A. G. Redfield, *Adv. Magn. Reson.* **1**, 1 (1965).
- [15] G Lindblad, *Commun. Math. Phys.* **48**, 119 (1976).
- [16] V. Gorini, A. Kossakowski, and E. C. G. Sudarshan, *J. Math. Phys.* **17**, 821 (1976).
- [17] J. M. Torres, *Phys. Rev. A* **89**, 052133 (2014).
- [18] M. Esposito, U. Harbola, and S. Mukamel, *Phys. Rev. B* **75**, 155316 (2007).
- [19] S. Ajisaka, F. Barra, C. Mejía-Monasterio, and T. Prosen, *Phys. Rev. B* **86**, 125111 (2012).
- [20] T. Prosen, *New J. Phys.* **10**, 043026 (2008).
- [21] T. Prosen, *J. Stat. Mech.* (2010) P07020.
- [22] M. Znidaric, *J. Phys. A* **43**, 415004 (2010).
- [23] S. Ajisaka, B. Zunkovic, and Y. Dubi, *Sci. Rep.* **5**, 8312 (2015).
- [24] S.-A. Biehs and G. S. Agarwal, *J. Opt. Soc. Am. B* **30**, 700 (2013).
- [25] A. Asadian, D. Manzano, M. Tiersch, and H. J. Briegel, *Phys. Rev. E* **87**, 012109 (2013).
- [26] A. Rivas and S. F. Hulega, *Open Quantum Systems* (Springer, Berlin, Heidelberg, 2012).
- [27] M. Bauer, Bachelor's thesis, University of Munich, 2011.
- [28] A. Levy and R. Kosloff, *Europhys. Lett.* **107**, 20004 (2014).
- [29] H. Wichterich, M. J. Henrich, H. P. Breuer, J. Gemmer, and M. Michel, *Phys. Rev. E* **76**, 031115 (2007).
- [30] J. Wu, *New J. Phys.* **12**, 083042 (2010).
- [31] R. A. Pepino, J. Cooper, D. Meiser, D. Z. Anderson, and M. J. Holland, *Phys. Rev. A* **82**, 013640 (2010).
- [32] K. Saito, S. Takesue, and S. Miyashita, *Phys. Rev. E* **61**, 2397 (2000).
- [33] K. Saito, *Europhys. Lett.* **61**, 34 (2003).
- [34] J. Wu and M. Berciu, *Phys. Rev. B* **83**, 214416 (2011).
- [35] B. Zunkovic and T. Prosen, in *Let's Face Chaos through Non-linear Dynamics: 8th International Summer School/Conference*, AIP Conf. Proc. No. 1468 (AIP, New York, 2012), p. 350.
- [36] U. Harbola, M. Esposito, and S. Mukamel, *Phys. Rev. B* **74**, 235309 (2006).
- [37] I. Kondov, U. Kleinekathöfer, and M. Schreiber, *J. Chem. Phys.* **114**, 1497 (2001).
- [38] I. Kondov, U. Kleinekathöfer, and M. Schreiber, *J. Chem. Phys.* **119**, 6635 (2003).
- [39] S. Anderloni, F. Benatti, and R. Floreanini, *J. Phys. A* **40**, 1625 (2007).
- [40] G. Argentieri, F. Benatti, R. Floreanini, and M. Pezzutto, *Europhys. Lett.* **107**, 50007 (2014).
- [41] J. Thingna, J. S. Wang, and P. Hänggi, *Phys. Rev. E* **88**, 052127 (2013).
- [42] P. R. Eastham, P. Kirton, H. M. Cammack, B. W. Lovett, and J. Keeling, [arXiv:1508.04744](https://arxiv.org/abs/1508.04744).
- [43] G. W. Ford, M. Kac, and P. Mazur, *J. Math. Phys.* **6**, 504 (1965).
- [44] A. Dhar and D. Sen, *Phys. Rev. B* **73**, 085119 (2006).
- [45] A. Dhar and D. Roy, *J. Stat. Phys.* **125**, 801 (2006).
- [46] A. Dhar, K. Saito, and P. Hänggi, *Phys. Rev. E* **85**, 011126 (2012).
- [47] H. J. Carmichael, *Statistical Methods in Quantum Optics I*, Theoretical and Mathematical Physics, 1st ed. (Springer-Verlag, Berlin, Heidelberg, 1999).
- [48] G. S. Agarwal, *Quantum Optics* (Cambridge University Press, Cambridge, 2013).
- [49] M. Znidaric, T. Prosen, G. Benenti, G. Casati, and D. Rossini, *Phys. Rev. E* **81**, 051135 (2010).
- [50] H. Spohn and J. L. Lebowitz, *Adv. Chem. Phys.* **38**, 109 (1978).
- [51] R. Dümcke and H. Spohn, *Z. Phys. B* **34**, 419 (1979).
- [52] N. Roch, M. E. Schwartz, F. Motzoi, C. Macklin, R. Vijay, A. W. Eddins, A. N. Korotov, K. B. Whaley, M. Sarovar, and I. Siddiqi, *Phys. Rev. Lett.* **112**, 170501 (2014).
- [53] C. Aron, M. Kulkarni, and H. E. Türeci, *Phys. Rev. A* **90**, 062305 (2014).
- [54] M. E. Schwartz, L. Martin, E. Flurin, C. Aron, M. Kulkarni, H. E. Türeci, and I. Siddiqi, [arXiv:1511.00702](https://arxiv.org/abs/1511.00702).
- [55] R. Mottl, F. Brennecke, K. Baumann, R. Landig, T. Donner, and T. Esslinger, *Science* **336**, 1570 (2012).
- [56] F. Brennecke, R. Mottl, K. Baumann, R. Landig, T. Donner, and T. Esslinger, *Proc. Natl. Acad. Sci. USA* **110**, 11763 (2013).
- [57] D. Porras, F. Marquardt, J. von Delft, and J. I. Cirac, *Phys. Rev. A* **78**, 010101(R) (2008).
- [58] R. Hartle, G. Cohen, D. R. Reichman, and A. J. Millis, *Phys. Rev. B* **88**, 235426 (2013).
- [59] R. Hartle and A. J. Millis, *Phys. Rev. B* **90**, 245426 (2014).
- [60] T. Prosen and B. Zunkovic, *New J. Phys.* **12**, 025016 (2010).
- [61] C. Aron, M. Kulkarni, and H. E. Türeci, *Phys. Rev. X* **6**, 011032 (2016).